

# Beyond Model Base Selection: Weaving Knowledge to Master Fine-grained Neural Network Design

Jiali Wang<sup>1</sup>, Hanmo Liu<sup>1,2</sup>, Shimin Di<sup>3</sup>, Zhili Wang<sup>1</sup>, Jiachuan Wang<sup>1</sup>, Lei Chen<sup>1,2</sup>, Xiaofang Zhou<sup>1</sup>

<sup>1</sup>The Hong Kong University of Science and Technology, Hong Kong SAR, China

<sup>2</sup>The Hong Kong University of Science and Technology (Guangzhou), Guangzhou, China

<sup>3</sup>Southeast University, Nanjing, China

jwangic@connect.ust.hk, hliubm@connect.ust.hk, shimin.di@seu.edu.cn, zwangeo@connect.ust.hk,

jwangey@connect.ust.hk, leichen@hkust-gz.edu.cn, zxf@cse.ust.hk

**Abstract**—Database systems have recently advocated for embedding machine learning (ML) capabilities, offering declarative model queries over large, managed model repositories, thereby circumventing the huge computational overhead of traditional ML-based algorithms in automated neural network model selection. Pioneering database studies aim to organize existing benchmark repositories as model bases (MB), querying them for the model records with the highest performance estimation metrics for given tasks. However, this static model selection practice overlooks the fine-grained, evolving relational dependencies between diverse task queries and model architecture variations, resulting in suboptimal matches and failing to further refine the model effectively. To fill the model refinement gap in database research, we propose M-DESIGN, a curated model knowledge base (MKB) pipeline for mastering neural network refinement by adaptively weaving prior insights about model architecture modification. First, we propose a knowledge weaving engine that reframes model refinement as an adaptive query problem over task metadata. Given a user’s task query, M-DESIGN quickly matches and iteratively refines candidate models by leveraging a graph-relational knowledge schema that explicitly encodes data properties, architecture variations, and pairwise performance deltas as joinable relations. This schema supports fine-grained relational analytics over architecture tweaks and drives a predictive query planner that can detect and adapt to out-of-distribution (OOD) tasks. We instantiate M-DESIGN for graph analytics tasks, where our model knowledge base enriches existing benchmarks with structured metadata covering 3 graph tasks and 22 graph datasets, contributing data records of 67,760 graph models. Empirical results demonstrate that M-DESIGN delivers the optimal model in 26 of 33 data-task combinations, significantly surpassing existing model selection methods under the same refinement budgets.

## I. INTRODUCTION

From perceptrons [1] to Transformers [2], the success of machine learning owes much to continuous advancements in neural network (NN) models [3]–[6]. Yet, the automatic selection of effective NN models for a specific analytics task has long relied on an expensive, trial-and-error process dominated by the machine learning (ML) community, where massive computational resources are repeatedly consumed to “reinvent the wheel.” A prominent example is Neural Architecture Search (NAS) [7]–[10], which exhaustively evaluates numerous candidate models for each new task, often redundantly repeating similar computations without effectively reusing well-performed models from similar tasks [11]. Specifically,

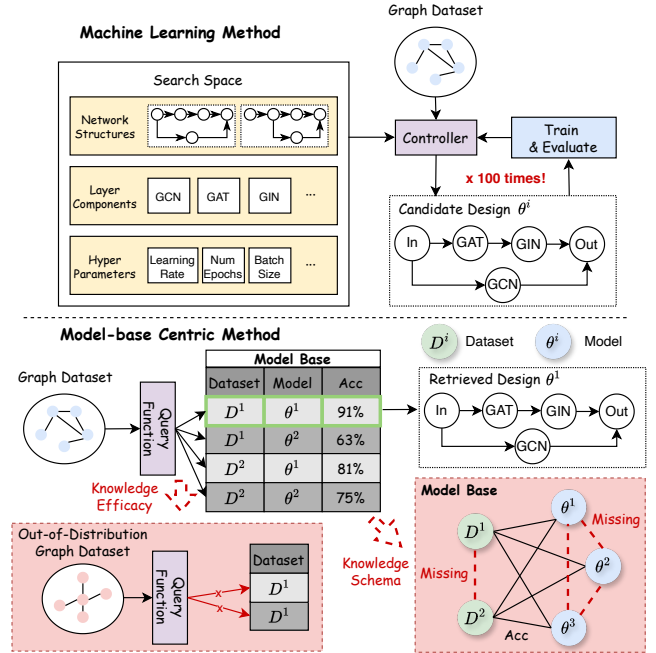


Fig. 1: Comparison between conventional ML-based methods and MB-centric methods, illustrating current limitations.

the fundamental inefficiency behind NN model selection lies in exploring the unknown and non-convex model-performance landscape [12], [13], which is hard for ML-based algorithms to fully capture the intricate correlation between model configurations and task performance without extensive searches.

In contrast, database research [14]–[20] has consistently advocated against redundant computations by championing structured reuse of historical model-performance records through a model base (MB) and declarative model queries [21], [22]. Pioneering database-centric efforts [23]–[26] emphasize systematically collecting, structuring, and querying model bases to retrieve model records with the highest performance estimation metrics for given tasks, thereby achieving reasonable performance without exhaustive searches. Recent advances like TRAILS [27] further integrate iterative model selection into database systems, striking a balance between efficient exploration and exploitation. Those MB-centric methods leverage relational constructs, such as structured user-defined func-

tions [28] and predictive analytics [29], over stored performance metrics to efficiently prune and select suitable candidate models, dramatically reducing selection latency and costs.

However, despite their efficiency gains, current MB-centric methods [27] often cannot detect and adapt to unseen tasks that deviate significantly from known distributions, resulting in suboptimal model selection and failing to further refine the model effectively. As shown in Fig. 1, we attribute the shortcomings of existing works from two perspectives: *Knowledge Efficacy* and *Knowledge Schema*. First, the *knowledge efficacy* issue highlights that existing methods primarily rely on constructing static or globally computed task-similarity views [30]–[32] over model bases to select models, largely neglecting the schema adaptability critical for accurate task query matching and effective model refinement. They typically lack sophisticated query understanding mechanisms for adaptively matching data-sensitive model architectures with diverse data specifications in task queries, providing minimal support for iteratively refining retrieved models. For example, given a graph analytics task, graph topology (e.g., homophily vs. heterophily) can drastically alter the preferred receptive field, which in turn influences the selection criteria of specific Graph Neural Network (GNN) models [33]. Consequently, models that excel on known tasks may fail catastrophically on structurally distinct, out-of-distribution (OOD) tasks (e.g., applying a GCN [5] to a heterophily graph). Notably, this difficulty is further compounded when current methods implicitly assume that their model bases have perfect validity and coverage. As a result, while these methods [27], [31] perform well on in-distribution tasks, their model refinement struggles with OOD cases due to reliance on invalid or insufficient model bases.

Besides, the *knowledge schema* issue in model refinement refers to the lack of a relational structure within existing model bases to enable fine-grained relational analytics over model architecture tweaks, which is fundamental to any MB-centric work but has been underestimated so far. First, most existing methods passively reuse NAS-style benchmarks [34], [35] that only provide static, flat model-performance tables. However, these benchmarks were not designed for the relational modeling of metadata that yields fine-grained insights into specific architecture modifications that impact performance outcomes across diverse tasks. Building upon those model bases, existing methods primarily rely on coarse-grained model knowledge retrieval [30], [31], directly selecting model-performance records as indivisible units. Moreover, they operate predominantly on model records from a single benchmark source [26] after constructing a static task-similarity view over the model base’s tables, which severely restricts their capacity to dynamically adapt knowledge based on new feedback during iterative refinement. As a result, these methods often converge prematurely and yield suboptimal models even after iterative model refinement, limiting their practical utility where precise and continuous task-model-performance alignment is essential.

To fill the model refinement gap in database research, we present M-DESIGN, a curated model knowledge base (MKB) pipeline for mastering neural network refinement by

adaptively weaving prior insights about model architecture modification. By simply querying and refining over stored metadata, our pipeline aims to select near-optimal models for unseen tasks within a limited refinement overhead. Regarding *knowledge efficacy*, we propose a knowledge weaving engine that reframes the complex model refinement as an adaptive query problem over task metadata, dynamically updating task-similarity views based on localized architecture modification gains. This pipeline lays a theoretical foundation for iterative model refinement by coordinating fine-grained metadata integration across multiple benchmark tasks. Furthermore, since the current *knowledge schema* is insufficient to support fine-grained relational analytics over architecture tweaks, we establish a graph-relational knowledge schema that encodes data properties, architecture variations, and pairwise performance deltas as explicit relations, enabling quick joins and analytical queries to instantiate localized modification-gain views. On top of our modification gain graphs, we construct performance estimators based on past benchmark records to serve as predictive query planners, enabling accurate performance estimation for unseen tasks. This significantly reduces the trial-and-error costs in OOD scenarios. To validate the effectiveness of M-DESIGN, we instantiate it by selecting GNNs for graph analytics tasks, building a model knowledge base that systematically encodes the relational dependencies between graph topology and GNN architectures. Our contributions are listed as follows:

- M-DESIGN fills a crucial gap in MB-centric model selection studies by directly harnessing a structured model knowledge base for model refinement. Our pipeline systematically structures prior model knowledge and adaptively manages it for declarative model modification queries, paving the way for a new database-centric paradigm in the field of automated NN model selection.
- To maximize the utilization of prior model knowledge, M-DESIGN novelly reframes the complex model refinement as optimizing task-similarity views based on localized architecture modification gains in an adaptive query engine, thus successfully upgrading the MB-centric paradigm from static lookups to adaptive refinement.
- M-DESIGN builds a graph-relational knowledge schema that explicitly models the diverse performance impact of architectural tweaks across tasks. The modification gain graph built from benchmarks can pre-train accurate predictive query planners, largely reducing the refinement costs of attempting candidate models on OOD tasks.
- Our knowledge base enriches the graph learning benchmark with 3 graph tasks and 22 datasets, contributing 67,760 graph models along with their performance. Empirical results demonstrate that M-DESIGN delivers optimal models in 26 of 33 data-task pairs, largely surpassing existing methods under the same refinement budgets.

## II. PRELIMINARIES

In this section, we first introduce the background and problem definition of different model selection methods in the

existing literature, followed by the definition of model knowledge base and its current deficiencies. Then, we formulate a general definition of the model refinement problem in Sec.II-C, serving as the foundation central to our M-DESIGN pipeline.

### A. Background and Problem Definition

**Model selection** refers to identifying the optimal neural network model configuration that maximizes performance (e.g., accuracy or AUC) on a given task and data. Formally, given a task dataset  $D$ , a search space of candidate models  $\Theta$ , and a performance evaluation function  $\mathcal{P}(\theta, D)$  for model  $\theta \in \Theta$ , model selection seeks the optimal model  $\theta^*$  defined as:

$$\theta^* = \operatorname{argmax}_{\theta \in \Theta} \mathcal{P}(\theta, D). \quad (1)$$

Traditionally, this problem is studied by the database community through in-database selection [27] and the machine learning community via Neural Architecture Search (NAS) [36], with a different focus on efficiency versus effectiveness.

**MB-centric methods** primarily seek efficiency by systematically collecting, structuring, and retrieving historical model-performance data from model bases. Pioneering systems [23], [24] primarily focus on organizing and querying model data to streamline experiment management and facilitate reproducibility. Rafiki [13] advances this approach by managing distributed training and hyperparameter tuning workflows through structured model data queries, significantly reducing redundant computational efforts. Other systems [22], [25], [37]–[39] further provide structured, database-oriented interfaces for efficient model selection, hyperparameter tuning, and resource scheduling, leveraging relational model data management and SQL-style declarative queries. Recently, TRAILS [27] introduced a two-phase model selection that integrates training-free and training-based model evaluation within database systems, thereby efficiently balancing exploration and exploitation while achieving Service-Level Objectives. Collectively, these database systems emphasize the power of structured model queries to mitigate redundant computations in model selection.

Recognizing the increasing complexity of unseen task environments and data sensitivity, recent database methods have started incorporating query understanding mechanisms to construct task-similarity views over multi-source model bases  $\mathcal{M}$  and selectively retrieve applicable models. The objective of the MB-centric model selection can be formally defined as:

$$\begin{aligned} \theta^* &= \operatorname{argmax}_{\theta \in \mathcal{M}} \mathcal{P}(\theta, D^u), \\ \mathcal{P}(\theta, D^u) &\propto \mathcal{S}(D^u, D^i) \odot \mathcal{P}(\theta, D^i), \end{aligned} \quad (2)$$

where  $\mathcal{S}(D^u, D^i)$  is the task-similarity views of  $\mathcal{M}$  between the unseen task  $D^u$  and benchmark task  $D^i$ .  $\propto$  represents that the query of selecting a well-performed model for  $D^u$  is mainly proportional to task-similarity view  $\mathcal{S}(D^u, D^i)$  and the model performance  $\mathcal{P}(\theta, D^i)$ .  $\odot$  indicates that some special operations on  $\mathcal{S}(D^u, D^i)$  and  $\mathcal{P}(\theta, D^i)$  in different works. As  $\mathcal{P}(\theta, D^i)$  is known in model bases, recent MB-centric solutions diverge in how to define and construct  $\mathcal{S}(D^u, D^i)$ :

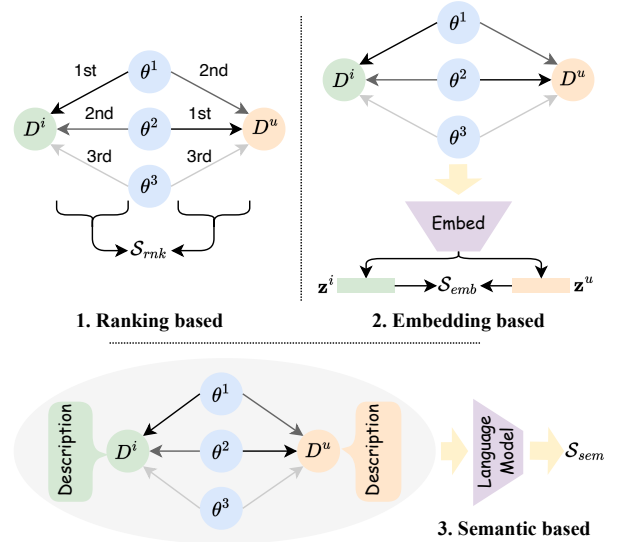


Fig. 2: Illustration of query understanding in model bases: 1) ranking-based, 2) embedding-based, and 3) semantic-based.

- 1) **Ranking-based** methods [26], [35] train a set of anchor models  $\Theta^a \subset \Theta$  across different benchmarks and unseen tasks and construct task-similarity views based on performance ranking correlations:  $\mathcal{S}_{\text{rnk}}(D^u, D^i) = \text{RankSim}(\mathcal{P}(\Theta^a, D^u), \mathcal{P}(\Theta^a, D^i))$ . They then directly select the best benchmark model as the optimum for  $D^u$ .
- 2) **Embedding-based** methods [30], [31], [40], [41] embed raw task and anchor models' features into latent spaces and construct task-similarity views by comparing task embeddings  $\mathbf{z}$ :  $\mathcal{S}_{\text{emb}}(D^u, D^i) = \text{Cosine}(\mathbf{z}^u, \mathbf{z}^i)$ .
- 3) **Semantic-based** methods [32], [42], [43] leverage large language models (LLMs) [44], [45] as meta-controllers  $\mathcal{LLM}(\cdot)$  to iteratively design models, correlating textual task descriptions with model insights from benchmark model bases and the literature. The task-similarity view is defined as  $\mathcal{S}_{\text{sem}}(D^u, D^i) = \mathcal{LLM}(D^u, D^i, \Theta^{i*})$ .

As shown in Eq. (2), current methods only retrieve coarse-grained performance records  $\mathcal{P}(\theta, D^i)$ , overlooking the incremental performance gains  $\Delta\mathcal{P}(\theta, \Delta\theta, D^i)$  brought by fine-grained modifications  $\Delta\theta$  to model architecture  $\theta$  across diverse tasks  $D^i$ . Besides, they primarily construct static task-similarity views over model bases to select models, implicitly assuming that the distribution of benchmark data generalizes to all new tasks. However, when selecting NN models for  $D^u$  that diverge from  $\mathcal{D}$  (i.e., the out-of-distribution scenario), the deviation in model-performance landscapes between  $D^u$  and  $\mathcal{D}$  will become too large for the retrieved model to be effective. **ML-based methods** explore a vast search space by iteratively sampling candidate models, evaluating them through training-based methods, and updating search strategies accordingly:

$$\theta^* = \operatorname{argmax}_{\theta \sim \pi_\alpha(\Theta)} \mathbb{E}[\mathcal{P}(\theta, D)], \quad (3)$$

where  $\pi_\alpha(\Theta)$  is the model sampling strategy. While those NAS methods [46]–[49] yield near-optimal solutions, they rely on repeated trials and can fail to converge under limited budgets [36], [50], [51]. Moreover, these approaches suffer from

stateless querying, as each NAS process operates independently for each task and does not leverage previously retrieved model-performance records from other tasks. This cold-start issue underlies their high resource demands, particularly when working with high-dimensional, non-convex spaces.

### B. Model Knowledge Base in Model Selection

To bypass the cold-start issue in model selection problem, the database community has treated prior model-performance records as a queryable model base  $\mathcal{M}$ . However, a higher-level model knowledge often refers to structured relations linking task datasets, model architectures, and performance outcomes:

$$\mathcal{K} : \mathcal{D} \times \Theta \rightarrow \mathcal{P}, \quad (4)$$

where task datasets  $\mathcal{D}$ , models  $\Theta$ , and performance metrics  $\mathcal{P}$  are systematically represented as relational schema entries. Acquiring such a model knowledge base  $\mathcal{K}$  allows us to predict promising model configurations on new tasks. Currently, such metadata is mainly presented as NAS-style benchmarks [34], which record model-performance mappings across diverse benchmark datasets in separate flat tables. However, such an unstructured model *knowledge schema* lacks fine-grained relationality and adaptability to support relational analytics over architecture tweaks important in effective model refinement:

- **Fine-grained Relationality:** As NAS-style benchmarks are developed for efficiently evaluating NAS methods, they lack a fine-grained relational structure that links diverse task queries with model architecture variations. The transferability of the model knowledge is thus limited.
- **Schema Adaptability:** Existing methods implicitly assume that unseen datasets always distribute similarly to known datasets  $D^u \sim \mathcal{D}$ . This assumption does not hold in real life, as deviations in topology, feature distributions, or task requirements can easily render unseen tasks OOD. Without mechanisms to detect and adapt to such distributional drift, existing model knowledge bases may provide invalid or harmful knowledge to unseen tasks.

### C. Model Refinement Problem Definition

As discussed in Sec. II-A, Sec. II-B, and Eq. (2), current MB-centric methods are constrained by the formulation of model knowledge and can only retrieve coarse-grained model-performance records  $\mathcal{P}(\theta, D^i)$  in a given benchmark, thus failing to refine the model effectively. To enable fine-grained analytics, we first formulate the model refinement problem as a sequential decision-making process [52] based on the **Architecture Modification Gains** obtained from testing models:

$$\Delta P_t^u(\Delta\theta) \leftarrow P(\theta_t + \Delta\theta, D^u) - P(\theta_t, D^u). \quad (5)$$

To integrate iterative model refinement capabilities directly within the model base, we formally define the **Model Refinement** problem as an MB query-driven optimization problem.

**Definition 1** (Model Refinement Problem). *Given an unseen task  $D^u$  and a curated model knowledge base  $\mathcal{K}$  comprising historical model evaluations across multiple known tasks, the*

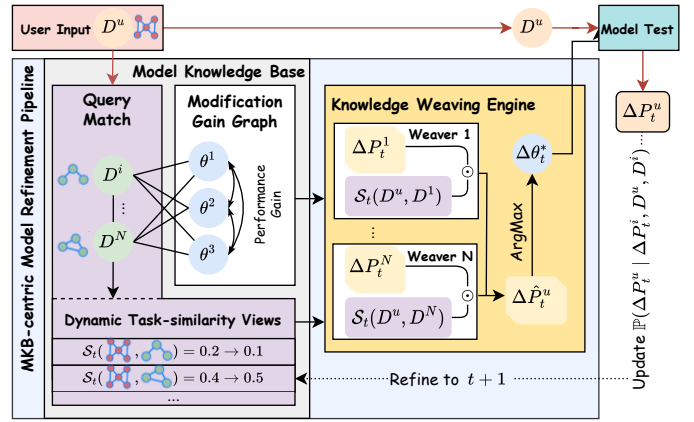


Fig. 3: Illustration of M-DESIGN: a model knowledge base (gray), together with the architecture modification gain graphs (white) and the knowledge weaving engine (yellow).

*refinement process seeks the optimal architecture modifications  $\Delta\theta_t^*$  maximizing expected performance gains at each step  $t$ :*

$$\Delta\theta_t^* = \operatorname{argmax}_{\Delta\theta \in \mathcal{K}} \mathbb{E}[\Delta P_t^u(\Delta\theta)] \quad (6)$$

*where the selection strategy  $\Delta\theta \in \mathcal{K}$  leverages knowledge base queries on structured task-model-performance metadata.*

This MKB-centric approach explicitly replaces the search controller with direct queries on a structured model knowledge base (MKB), enabling effective, query-driven refinement. The challenge is that the architecture modification gain  $\Delta P_t^u(\Delta\theta)$  remains unobservable without testing models, and the optimal modification  $\Delta\theta_t^*$  for each iteration  $t$  is unknown in advance.

## III. ARCHITECTURE KNOWLEDGE WEAVING

To address the model refinement challenge behind Def. (1), we present M-DESIGN, a curated model knowledge base pipeline that adaptively weaves fine-grained prior insights about model architecture modification. In this section, we first lay a theoretical foundation for iterative model refinement by coordinating fine-grained metadata integration across multiple benchmark tasks. By reframing the complex model refinement as an adaptive query problem over task metadata, we then propose a knowledge weaving engine that dynamically updates task-similarity views of the model knowledge base based on localized architecture modification gains, thereby enabling adaptive task query matching and effective model refinement with high *knowledge efficacy*. Our pipeline is in Algo. 1.

### A. Fine-grained Knowledge Weaving for Model Refinement

The major challenge in solving Eq. (6) arises from the lack of prior access to true modification gains  $\Delta P_t^u(\Delta\theta)$  on the unseen task  $D^u$  before testing, making direct optimization intractable. Our key motivation is that tasks exhibiting consistent modification gains for local architecture tweaks likely share similar modification landscapes. Therefore, we propose to approximate  $\Delta P_t^u(\Delta\theta)$  by weaving observed modification gains  $\Delta P_t^i(\Delta\theta)$  from benchmark tasks  $\mathcal{D}^b = \{D^i\}_{i=1}^N$ . Intuitively, the true modification gain on  $D^u$  is linearly correlated to the

observed modification gain on  $D^i$ , conditioned by the high task similarity, which is formally defined as follows:

**Definition 2** (Task Similarity via Modification Consistency). *Let  $D^u$  be an unseen task, and let  $\mathcal{D}^b = \{D^i\}_{i=1}^N$  be a set of benchmark tasks with known performance over a model space  $\Theta$ . For a given model  $\theta_t \in \Theta$  and any 1-hop modification  $\Delta\theta_t$ , we define task similarity  $\mathcal{S}(\cdot, \cdot)$  such that if  $\mathcal{S}(D^u, D^i)$  over a threshold  $\delta$ , then the performance gain on  $D^u$  and  $D^i$  is linearly consistent:*

$$\begin{aligned} \mathbb{E}[\Delta P_t^u(\Delta\theta) \mid \Delta P_t^i(\Delta\theta), \mathcal{S}(D^u, D^i) \geq \delta] \\ = \gamma_{i,t} \Delta P_t^i(\Delta\theta) + \epsilon_{i,t}. \end{aligned} \quad (7)$$

where  $\Delta P_t^i(\Delta\theta) = P(\theta_t + \Delta\theta, D^i) - P(\theta_t, D^i)$ ,  $\gamma_{i,t}$  is a scaling factor representing the expected transferability from  $D^i$  to  $D^u$ , and  $\epsilon_{i,t}$  captures unmodeled discrepancies.

Empirically validated in Sec. V-C1, this formulation implies that task model queries with high task similarity exhibit predictable modification behavior, enabling accurate performance forecasting without direct testing. To fully exploit this idea, we theoretically reformulate the problem in Def. (1) as an adaptive query problem over task-similarity views of the model knowledge base  $\mathcal{K}$  by weaving fine-grained modification knowledge  $\Delta P_t^i(\Delta\theta)$  across the known benchmark tasks in  $\mathcal{K}$ :

**Definition 3** (Knowledge Weaving for Model Refinement). *Given an unseen task  $D^u$ , a current model  $\theta_t$ , and a curated model knowledge base  $\mathcal{K}$  with task-similarity views  $\mathcal{S}(\cdot, \cdot)$  covering historical performance records of architecture modifications across multiple benchmark tasks  $\mathcal{D}^b = \{D^i\}_{i=1}^N$ , the adaptive query selects the optimal architecture modification  $\Delta\theta_t^*$  maximizing the woven performance gain at iteration  $t$ :*

$$\Delta\theta_t^* = \operatorname{argmax}_{\Delta\theta \in \mathcal{K}_s} \sum_{i=1}^N \mathcal{S}(D^u, D^i) \cdot \Delta P_t^i(\Delta\theta), \quad (8)$$

where the performance gains  $\Delta P_t^i(\Delta\theta)$  are known on  $D^i$  and retrieved directly from structured model knowledge base  $\mathcal{K}$ .

We further prove that this problem reformulation is valid:

**Theorem 1.** *Given a task-similarity view over  $\mathcal{K}$  that satisfies Def. (2), the general model refinement problem in Def. (1) admits the equivalent reformulation in Def. (3).*

*Proof.* We start by considering the probability that a performance improvement  $\Delta\mathcal{P}$  observed on a benchmark task  $D^i$  is relevant to  $D^u$ . This is captured by the posterior probability  $\mathbb{P}(D^i \mid D^u)$ . The task-similarity view  $\mathcal{S}(D^u, D^i)$  defined in Eq. (14) satisfies Def. (2) and is proportional to  $\mathbb{P}(D^i \mid D^u)$ :

$$\mathbb{P}(D^i \mid D^u) = \frac{\mathcal{S}(D^u, D^i)}{\sum_{j=1}^N \mathcal{S}(D^u, D^j)}, \sum_{i=1}^N \mathbb{P}(D^i \mid D^u) = 1 \quad (9)$$

Starting from the expected performance improvement on  $D^u$ :

$$\mathbb{E}[\Delta\mathcal{P}(\theta_t + \Delta\theta, D^u) \mid \theta_t] = \int \Delta\mathcal{P} \cdot \mathbb{P}(\Delta\mathcal{P} \mid D^u) d\Delta\mathcal{P} \quad (10)$$

Since we cannot access  $\mathbb{P}(\Delta\mathcal{P} \mid D^u)$  directly, we approximate it using known distributions from benchmarks:

$$\mathbb{P}(\Delta\mathcal{P} \mid D^u) \approx \sum_{i=1}^N \mathbb{P}(D^i \mid D^u) \cdot \mathbb{P}(\Delta\mathcal{P} \mid D^i) \quad (11)$$

Substituting the approximation into the expectation gives:

$$\begin{aligned} \mathbb{E}[\Delta\mathcal{P}(\theta_t + \Delta\theta, D^u) \mid \theta_t] \\ \approx \sum_{i=1}^N \mathbb{P}(D^i \mid D^u) \int \Delta\mathcal{P} \cdot \mathbb{P}(\Delta\mathcal{P} \mid D^i) d\Delta\mathcal{P} \\ \approx \sum_{i=1}^N \mathbb{P}(D^i \mid D^u) \cdot \mathbb{E}[\Delta\mathcal{P}(\theta_t + \Delta\theta, D^i) \mid \theta_t] \end{aligned} \quad (12)$$

As performance improvements  $\Delta\mathcal{P}(\theta_t + \Delta\theta, D^i)$  are known in the knowledge base, we access them via deterministic queries under task-similarity views, where  $Z = \sum_{j=1}^N \mathcal{S}(D^u, D^j)$ :

$$\begin{aligned} \mathbb{E}[\Delta\mathcal{P}(\theta_t + \Delta\theta, D^u) \mid \theta_t] \\ \approx \sum_{i=1}^N \mathbb{P}(D^i \mid D^u) [\mathcal{P}(\theta_t + \Delta\theta, D^i) - \mathcal{P}(\theta_t, D^i)] \\ \approx \frac{1}{Z} \sum_{i=1}^N \mathcal{S}(D^u, D^i) [\mathcal{P}(\theta_t + \Delta\theta, D^i) - \mathcal{P}(\theta_t, D^i)] \end{aligned} \quad (13)$$

Finally, when the task-similarity views are pre-normalized so that  $Z = 1$ , this reduces exactly to our adaptive query form.  $\square$

### B. Adaptive Query via Dynamic Task-Similarity Views

While the task similarity definition in Def. (2) enables fine-grained knowledge weaving in Def. (3) to effectively approximate the model refinement objective in Def. (1), we empirically reveal (in Sec. V-C2) that modification gains can vary drastically across different regions of the landscape, causing global or static task-similarity views in Eq. (2) to fail.

To address this challenge, we introduce a dynamic task-similarity view  $\mathcal{S}_t(\cdot, \cdot)$  to capture the local modification consistency in real-time using Bayesian inference [53]. This adaptive schema ensures that if new evidence contradicts the initial guess that  $D^i$  is akin to  $D^u$ , the posterior  $\mathcal{S}_t$  gradually down-weights  $D^i$  to avoid overconfidence. Specifically, by Bayes' rule, we treat  $\mathcal{S}_t(D^u, D^i)$  as the updated belief about the local similarity and validity of knowledge transfer between  $D^u$  and  $D^i$ , adjusting its probability based on new observations  $\Delta P_t^u$ :

$$\mathcal{S}_t(D^u, D^i) = \frac{\mathbb{P}(\Delta P_t^u \mid \Delta P_t^i, D^u, D^i) \cdot \mathcal{S}_{t-1}(D^u, D^i)}{\sum_{j=1}^N \mathbb{P}(\Delta P_t^u \mid \Delta P_t^j, D^u, D^j) \cdot \mathcal{S}_{t-1}(D^u, D^j)} \quad (14)$$

where  $\mathbb{P}(\Delta P_t^u \mid \Delta P_t^i, D^u, D^i)$  is the likelihood of observing  $\Delta P_t^u$  on  $D^u$  given  $\Delta P_t^i$ , and  $\mathcal{S}_{t-1}(D^u, D^i)$  is the prior represented by task similarity from the last iteration. By Def. (2), for a high-similarity benchmark task  $D^i$  with  $\mathcal{S}(D^u, D^i) \geq \delta$ , we choose to model the relationship between  $\Delta P_t^u$  and  $\Delta P_t^i$  as a Gaussian distribution with mean  $\gamma_{i,t} \Delta P_t^i$  and variance  $\sigma^2$ . The modeling of Gaussian likelihood, validated in Sec. V-C1,

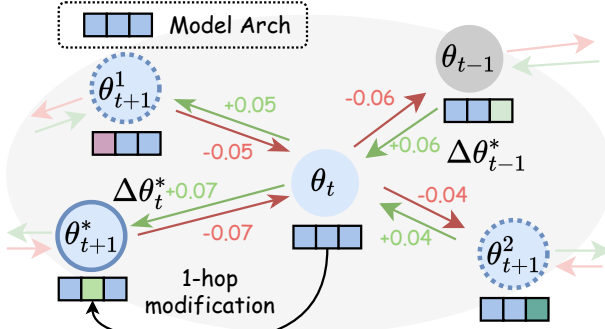


Fig. 4: Illustration on the architecture modification gain graph. Edges are noted with performance gains.

enables smooth probabilistic updates in task-similarity views, preventing abrupt changes that could lead to instability:

$$\mathbb{P}(\Delta P_t^u | \Delta P_t^i, \gamma_{i,t}, \sigma^2) = \frac{1}{\sqrt{2\pi\sigma^2}} \exp\left(-\frac{(\Delta P_t^u - \gamma_{i,t}\Delta P_t^i)^2}{2\sigma^2}\right), \quad (15)$$

where  $\gamma_{i,t}$  and  $\sigma^2$  are estimated using the history of new observations  $(\Delta P^u, \Delta P^i)$  up to iteration  $t$ , applying sliding windows of size  $w$  to control the locality. By iteratively updating  $\gamma_{i,t}$  and  $\sigma^2$ , task-similarity views of model knowledge base are dynamically adjusted to reflect local consistency in architecture modification gains. As illustrated in Fig. 3, this enables an adaptive query engine that coordinates fine-grained metadata integration across diverse benchmark tasks, approximating modification gains on unseen tasks and maximizing the expected performance improvement at each step.

#### IV. GRAPH-RELATIONAL MODEL KNOWLEDGE BASE

The architecture knowledge weaving in Sec. III lays a theoretical foundation for harnessing the model knowledge base in model refinement. However, as discussed in Sec. II-B, a critical but overlooked factor is the *knowledge schema* and the adaptability issue of the stored knowledge itself. Intuitively, current benchmarks only record the performance outcome of the model  $\mathcal{P}(\theta_t, D^i)$ , i.e., precisely modeling  $\Delta P_t^i(\Delta\theta)$  in Def. (3) is still hard. To bridge these gaps, we introduce a graph-relational knowledge schema that encodes data properties, architecture variations, and pairwise performance deltas as explicit relations, enabling quick joins and analytical queries. To instantiate localized modification-gain views, we build architecture modification gain graphs in the model knowledge base to support the pre-training of GNN-based performance estimators, serving as accurate predictive query planners.

##### A. Data Model and Logical Schema

In our model knowledge base, we organize all benchmark records and modification gain graphs into three core relations:

- **Tasks:**  $(\text{task\_id}, \text{dataset\_id}, \text{feature\_vector}, \text{task\_type}, \dots)$ —stores each task’s ID and its pre-computed statistical data properties (e.g. homophily, density).
- **Architectures:**  $(\text{arch\_id}, \text{design\_tuple}, \dots)$ —an entry per unique model architecture, where design choices and hyperparameters are encoded in  $\text{design\_tuple}$ .

#### Algorithm 1: M-DESIGN: Adaptive Knowledge Weaving for MKB-centric Model Refinement

**Input** : Unseen task  $D^u$ , initial model architecture  $\theta_0$ , initial task-similarity views  $\{\mathcal{S}_0(D^u, D^i)\}_{i=1}^N$ , maximum iterations  $T$ , and OOD threshold  $\beta$

**Output** : Near-optimal model architecture  $\theta^*$  for  $D^u$

```

1 for  $t = 0$  to  $T - 1$  do
2   for each 1-hop candidate modification  $\Delta\theta_t \in \mathcal{G}_\Delta^u(\theta_t)$  do
3     Compute weaving gain:  $\hat{\Delta}\mathcal{P}(\theta_t, \Delta\theta_t, D^u) \leftarrow$ 
4        $\sum_{i=1}^N \mathcal{S}_t(D^u, D^i) \cdot \hat{\Delta}P_t^i(\Delta\theta_t)$ ; // OOD flag
5   end
6    $\Delta\theta_t^* \leftarrow \arg \max_{\Delta\theta_t \in \mathcal{G}_\Delta^u(\theta_t)} \hat{\Delta}\mathcal{P}(\theta_t, \Delta\theta_t, D^u)$ ;
7    $\theta_{t+1} \leftarrow \theta_t + \Delta\theta_t^*$ ; Evaluate  $\theta_{t+1}$  on  $D^u$  to obtain the
8     actual performance gain  $\Delta P_t^u$  and replace  $\theta^*$  if better;
9   for each benchmark task  $D^i \in \mathcal{D}^b$  do
10    Compute likelihood  $L_i$ , controlled by a sliding
11    window of size  $w$  over past  $\gamma$  and  $\sigma^2$ :
12     $L_i = \frac{1}{\sqrt{2\pi\sigma^2}} \exp\left(-\frac{(\Delta P_t^u - \gamma_{i,t}\Delta P_t^i)^2}{2\sigma^2}\right)$ 
13  end
14  for each benchmark task  $D^i \in \mathcal{D}^b$  do
15    Update task-similarity views using Bayes’ rule:
16     $\mathcal{S}_t(D^u, D^i) \leftarrow \frac{L_i \mathcal{S}_{t-1}(D^u, D^i)}{\sum_{j=1}^N L_j \mathcal{S}_{t-1}(D^u, D^j)}$ 
17    if  $\mathcal{S}_t(D^u, D^i) < \beta$ ; // Low similarity
18    then
19      Flag  $D^i$  as OOD;
20      Update predictive query planner for  $D^i$ ;
21  end
22  Add  $((\theta_t, \Delta\theta_t^*), \Delta P_t^u)$  to replay buffer  $R$ ;
23 end
24 return  $\theta^*$ ;

```

- **Modification Gains:**  $(\text{task\_id}, \text{arch\_from}, \text{arch\_to}, \text{gain})$ —a pairwise relation capturing every 1-hop architecture tweak ( $\text{arch\_from} \rightarrow \text{arch\_to}$ ) along with the measured performance gain on the task.

All three relations are linked by foreign keys ( $\text{task\_id}$ ,  $\text{arch\_id}$ ), and these tables form our logical schema for both static lookup and adaptive refinement.

##### B. Architecture Modification Gain Graph

A major limitation of existing model bases is their reliance on flat model-performance records  $(\theta, \mathcal{P}(\theta, D^i))$  from NAS benchmarks [34], which lack the ability to support fine-grained relational analytics. Therefore, we propose **Architecture Modification Gain Graph**  $G_\Delta^i$  as a structured representation of historical model refinement trajectories on each benchmark task  $D^i$ . As shown in Fig. 4, each node represents a concrete and unique model architecture. Each edge represents 1-hop architecture modifications  $\Delta\theta$  between models, e.g., change the activation function from ReLU to LeakyReLU. The edge is labeled with known performance gain  $\Delta P_t^i(\Delta\theta)$ . Note that all edges are bidirectional, e.g., a 5% increase in accuracy from one modification indicates a 5% decrease from the reverse modification. Unlike existing model bases, our modification gain graphs encode architecture variations

TABLE I: The complete model space in our model knowledge base. Bolded choices have been recorded in the released version.

Type	Design Dimension	Candidate-set $O$
Pre-MPNN	Transformation $\mathbf{f}_\theta$	$O_{f_\theta} = \{\text{MLP (\#layer: 1, 2, 3)}\}$
	Neighbor mechanism $N_k(v)$	$O_N = \{\text{first\_order, high\_order, attr\_rewire, diff\_rewire, PE/SE\_rewire}\}$
Intra-layer	Edge weight $c_{uv}^k$	$O_e = \{\text{non\_norm, sys\_norm, rw\_norm, self\_gating, rel\_lepe, rel\_rwpe}\}$
	Intra aggregation $intra\_agg_k$	$O_{intra\_agg} = \{\text{sum, mean, max, min}\}$
	Activation $\sigma$	$O_\sigma = \{\text{relu, prelu, swish}\}$
	Dropout $r_d$	$O_{r_d} = \{\mathbf{0}, 0.3, 0.5, 0.6\}$
	Combination $comb_k$	$O_{comb} = \{\text{sum, concat}\}$
	Inter-layer	Message passing layers $n_l$
Inter aggregation $inter\_agg$		$O_{inter\_agg} = \{\text{concat, last, mean, decay, gpr, lstm\_att, gating, skip\_sum, skip\_cat}\}$
Post-MPNN	Transformation $\mathbf{f}_\kappa$	$O_{f_\kappa} = \{\text{MLP (\#layer: 1, 2, 3)}\}$
	Edge Decoding $\mathbf{f}_d$	$O_{f_d} = \{\text{dot, cosine\_similarity, concat}\}$
	Graph Pooling $\mathbf{f}_p$	$O_{f_p} = \{\text{add, mean, max}\}$
Training	Learning rate $r_l$	$O_{r_l} = \{0.1, \mathbf{0.01}, 0.001\}$
	Optimizer $opt$	$O_{opt} = \{\text{sgd, adam}\}$
	Epochs $n_e$	$O_{n_e} = \{100, 200, \mathbf{300}, 400, 500\}$

TABLE II: Comparison of the optimal model in our knowledge base with NAS-Bench-Graph (NBG) on overlapping datasets.

Method	Cora	CiteSeer	PubMed	CS	Computers	Photo
NBG [34]	86.22	74.03	88.12	91.26	85.58	92.78
M-DESIGN	<b>88.50</b>	<b>74.59</b>	<b>89.08</b>	<b>95.33</b>	<b>89.59</b>	<b>94.75</b>

and pairwise performance deltas as explicit relations, enabling analytical queries to model localized modification gains.

### C. OOD Adaptation via Predictive Query Planner

A key challenge in MB-centric model selection is the risk of negative transfer when the unseen task  $D^u$  deviates significantly from existing benchmarks  $\mathcal{D}^b$ . In Sec. IV-B, the modification gain graph records the architecture modification along with performance improvements, which forms a foundation for predictive analytics over relational metadata. Thus, M-DESIGN leverages such graphs and pre-trains GNN-based performance estimators on past benchmark records to serve as predictive query planners, enabling accurate performance estimation on unseen tasks, particularly in OOD scenarios.

First, by Def. (2), we identify that  $D^u$  is OOD relative to  $D^i$  if the dynamic similarity  $\mathcal{S}_t(D^u, D^i)$  remains persistently low (e.g., 0.2 after normalization). In that case, relying on direct, static retrievals from such a benchmark may degrade predictive performance in Def. (3) because the linearity and Gaussian assumption in Eq. (15) may not hold. To mitigate OOD effects by smoothing predictions and adapting to distribution shifts, we augment each benchmark task in  $\mathcal{K}$  with an edge regression GNN (e.g., EdgeConv [54]) pre-trained on the modification gain graph  $\mathcal{G}_\Delta^i$  by minimizing L1 loss based on modification gain  $\Delta P^i(\Delta\theta)$ . Evaluated by Wasserstein distance [55], the estimator learns to execute predictive analytics on modification gains  $\Delta P_t^i(\Delta\theta)$  given a model pair  $(\theta_t, \theta_t + \Delta\theta_t)$ .

During model refinement, those estimators can be further fine-tuned using a replay buffer  $R$ , incorporating past benchmark records and newly observed  $((\theta_t, \theta_t + \Delta\theta_t^*), \Delta P_t^u(\Delta\theta))$  pairs from the optimization trajectory. On demand, this online learning gradually shifts the estimator’s knowledge distribution to better estimate  $\Delta P_t^u$  for the unseen task  $D^u$ . Once  $D^i$  is OOD-flagged, the estimator of  $D^i$  will supply an estimated

gain  $\Delta \hat{P}_t^i(\Delta\theta)$  to the knowledge weaving engine defined in Def. (3), functioning as a predictive query planner of OOD:

$$\Delta P_t^u(\Delta\theta) \approx \sum_{i=1}^N \mathcal{S}(D^u, D^i) \Delta \hat{P}_t^i(\Delta\theta), \quad (16)$$

This ensures that even if  $D^i$  was initially far from  $D^u$ , our model knowledge base remains adaptive—gradually shifting the learned distribution to better reflect the unseen distribution. For the in-distribution benchmarks that are not OOD-flagged, the retrieval pipeline of modification gains remains direct.

### D. Model Knowledge Base for Graph Analytics Tasks

Graph data is a notoriously data-sensitive domain for model selection because the topological diversity in graph data has a larger impact on architecture performance than in other data modalities [26]. There does not exist a universal GNN architecture that can handle all graph data effectively. Thus, we instantiate M-DESIGN in selecting GNNs and construct our model knowledge base, which enriches the existing benchmarks with 3 task types and 22 graph datasets, contributing 67,760 more models along with their performance records.

- 1) *Broader Graph Tasks and Detailed Topology*: We pioneer an extension beyond the node classification task in graph learning to include both link prediction and graph classification tasks—covering 11 representative datasets for each task (see Tab. IV)—and explicitly document rich graph topology that may affect model selection [32], [33].
- 2) *Specialized Model Space*: We focus on fine-grained architecture dimensions (6,160 unique models from Tab. I) grounded in message-passing schema [26], [33], benchmarking higher performance ceiling compared to NAS benchmarks [35] (shown in Tab. II).
- 3) *Data-driven Architecture Insights*: Unlike existing NAS benchmarks, which store raw performance records without explainability, our model knowledge base implicitly encodes correlations between graph topology (e.g., homophily ratio), GNN architecture choices (e.g., aggregation), and expected performance impacts.

In our implementation, M-DESIGN can quickly initialize task-similarity views  $\mathcal{S}_0(D^u, D^i)$  before any direct model testing on  $D^u$  by directly analyzing these underlying correlations

TABLE III: Comparison of ML-based and MB-centric model selection methods under a maximum search budget of 100 model-testings across 11 node classification datasets. The best results are **bolded**. \* marks reaching global optimum.

Method	Actor	Computers	Photo	CiteSeer	CS	Cora	Cornell	DBLP	PubMed	Texas	Wisconsin
<b>Space Optimum</b>	<b>34.89</b>	<b>89.59</b>	<b>94.75</b>	<b>74.59</b>	<b>95.33</b>	<b>88.50</b>	<b>77.48</b>	<b>84.29</b>	<b>89.08</b>	<b>84.68</b>	<b>91.33</b>
Random	33.98	88.25	94.28	73.84	94.96	87.84	74.96	83.44	88.46	80.63	89.93
RL	33.95	88.25	94.37	73.88	95.02	88.01	74.87	83.40	88.58	81.62	89.73
EA	33.73	88.28	94.45	73.93	94.94	87.90	74.24	83.66	88.42	82.43	89.20
GraphNAS	34.11	87.94	94.38	73.89	94.90	88.01	74.60	83.40	88.58	81.98	89.87
Auto-GNN	33.71	87.59	94.46	74.14	95.15	87.94	74.51	83.69	88.38	81.71	89.60
GraphGym	32.72	82.57	93.53	72.68	94.71	87.95	69.37	82.54	87.61	74.77	83.33
NAS-Bench-Graph	32.17	82.57	93.70	65.67	93.88	88.07	69.37	83.47	88.66	74.77	86.67
KBG	32.72	87.38	94.53	74.23	94.71	87.95	69.37	83.47	88.15	74.77	86.67
AutoTransfer	33.97	87.72	94.62	73.89	95.16	<b>88.50*</b>	76.58	83.59	<b>89.08*</b>	78.38	88.67
DesiGNN	34.43	88.40	94.60	74.54	95.03	88.34	75.50	<b>84.29*</b>	<b>89.08*</b>	81.80	90.66
<b>M-DESIGN</b>	<b>34.89*</b>	<b>89.22</b>	<b>94.75*</b>	<b>74.59*</b>	<b>95.33*</b>	<b>88.50*</b>	<b>77.48*</b>	<b>84.29*</b>	<b>89.08*</b>	<b>83.79</b>	<b>91.33*</b>

TABLE IV: Benchmark datasets statistics in knowledge base.

Dataset	#Graph	#Node	#Edge	#Feature	#Class	Task
Actor	1	7,600	30,019	932	5	Node/Link
Computers	1	13,752	491,722	767	10	Node/Link
Photo	1	7,650	238,162	745	8	Node/Link
CiteSeer	1	3,312	4,715	3,703	6	Node/Link
CS	1	18,333	163,788	6,805	15	Node/Link
Cora	1	2,708	5,429	1,433	7	Node/Link
Cornell	1	183	298	1,703	5	Node/Link
DBLP	1	17,716	105,734	1,639	4	Node/Link
PubMed	1	19,717	88,648	500	3	Node/Link
Texas	1	183	325	1,703	5	Node/Link
Wisconsin	1	251	515	1,703	5	Node/Link
COX2	467	41.2	43.5	35	2	Graph
DD	1,178	284.3	715.7	89	2	Graph
IMDB-B.	1,000	19.8	96.5	136	2	Graph
IMDB-M.	1,500	13.0	65.9	89	3	Graph
NCI1	4,110	29.9	32.3	37	2	Graph
NCI109	4,127	29.7	32.1	38	2	Graph
PROTEINS	1,113	39.1	72.8	3	2	Graph
PTC_FM	349	14.1	14.5	18	2	Graph
PTC_FR	351	14.6	15.0	19	2	Graph
PTC_MM	336	14.0	14.3	20	2	Graph
PTC_MR	344	14.3	14.7	18	2	Graph

using large language models [32] or statistical methods like 1) average Kendall’s  $\tau$  rank correlation over data statistic or 2) Principal Component Analysis (PCA) [56]. To obtain an initial model, we take the weighted average of the best-performing models’ architecture choices on each benchmark dataset, in which the weights are the initial task-similarity views. By combining these, our model knowledge base is not simply a static collection of  $(\theta, \mathcal{P}(\theta, D^i))$  pairs; rather, it is a structured knowledge schema of modification gain graphs that enables more proficient utilization of prior model selection insight.

## V. EXPERIMENTS

### A. Experimental Settings

**Tasks and Datasets.** We conduct our experiments based on our graph instantiation in Sec. IV-D. In total, there are 3 task types, 22 datasets, and 33 data-task pairs, all with classical preprocessing [26]. These datasets comprehensively represent diverse graph topologies, node homophily, task complexities, etc. The basic dataset statistics are summarized in Tab. IV.

**Baselines.** We compare with 3 categories of 10 baselines:

- 1) **ML-based Methods:** NAS approaches that search models for tasks from scratch, including Random Search [57], Reinforcement Learning (RL) [47], Evolutionary Algorithms (EA) [58], GraphNAS [59], and Auto-GNN [10].
- 2) **MB-centric Model Selection:** Model bases that rely on static model selection from similar tasks, including GraphGym [26], NAS-Bench-Graph [35], and KBG [30].
- 3) **MB-centric Model Refinement:** SOTA methods that integrate iterative search into MB-centric model selection, including AutoTransfer [31] and DesiGNN [32].

We equip all the baselines with the same model space defined in our knowledge base for a fair comparison of design efficacy.

**Evaluation Metrics.** We evaluate the model selection (1) *effectiveness* with the classification accuracy or AUC-ROC on all data-task pairs under a maximum search budget of 100 model-testings and (2) *refinement efficiency* with the number of model-testings (i.e., the basic time unit in the benchmarking setting) required for methods to achieve the target performance level, i.e., the halfway performance marked by running 50 iterations of M-DESIGN on the node classification task.

**Implementation Details.** M-DESIGN is implemented under SQLite, PyTorch [60], and LangChain [61] (GPT-4o), running using a single RTX 3080 GPU. Our data collection pipeline for the released model knowledge base is built upon the GraphGym platform [26], and our model design space is detailed in Tab. I. The modification gain graphs of benchmark datasets are structured following the data standard in PyG [62]. We implemented GNN-based predictive query planners with two layers and a hidden dimension of 64 using PyG’s EdgeConv. To prevent data leakage from the model knowledge base, we excluded the unseen dataset from the benchmark list during evaluation. All results are averaged over 10 repeated trials.

### B. Main Results on Model Selection Efficacy

We evaluate M-DESIGN’s model refinement efficacy by assessing its ability to select near-optimal models for unseen tasks within a limited refinement budget.

**Effectiveness** is the primary goal of model refinement tasks. We compare M-DESIGN against all baselines by evaluating

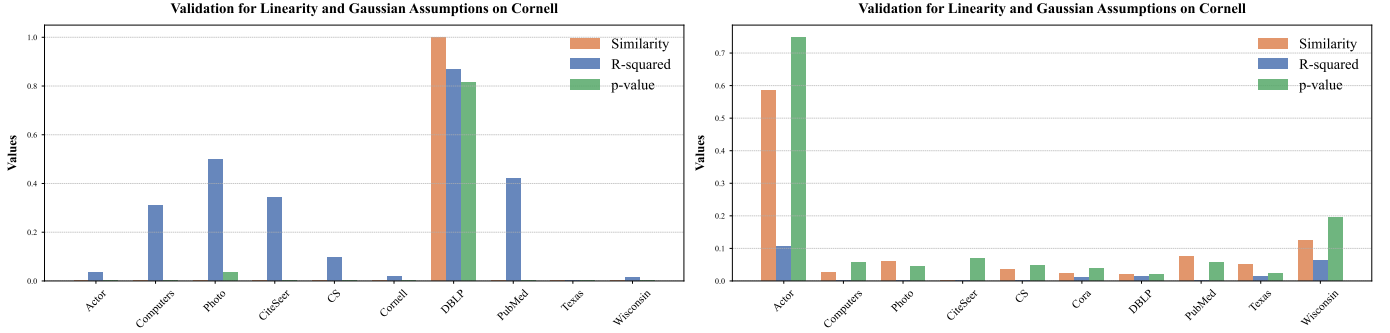


Fig. 5: Bar charts showing the empirical supports for the theoretical assumption on Cora and Cornell. Each benchmark dataset has three bars: our stabilized task-similarity views, R-squared (Linearity), and Shapiro-Wilk p-value (Gaussian).

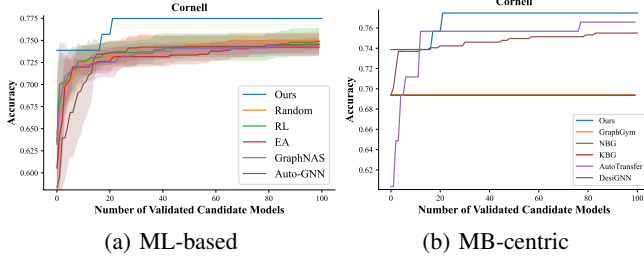


Fig. 6: Long-run model refinement trajectories of M-DESIGN compared to ML-based and MB-centric methods on Cornell.

the task performance of their selected models, whose results are shown in Tab. III (link prediction and graph classification results are shown in Tab. VII and Tab. VIII). Across 33 data-task pairs, MB-centric model selection methods tend to be inferior to ML-based methods, as they often struggle to adapt effectively to unseen tasks. MB-centric model refinement methods overcome this limitation with better refining strategies, yet their static usage of model bases often leads to premature convergence to local optima. M-DESIGN further dynamically adapts the model knowledge base to unseen tasks, achieving the global optimum of the model space in 26 out of 33 data-task pairs and consistently outperforming all baselines. Notably, even in challenging datasets such as Computers and Texas, it still ranks as the second-best model over the space, demonstrating its robustness across diverse graph topologies.

**Refinement Efficiency** remains an essential goal even after trading off iterative testing costs for effective outcomes. In practice, the average computation time added by M-DESIGN’s MKB operation is  $<0.3080$  seconds per iteration, and  $<0.4399$  when activating OOD adaptation, which is negligible compared to model-testing time (e.g.,  $\sim 30$  seconds each for testing a model on the Actor dataset with an RTX 3080 GPU).

As we conducted our experiments under the benchmarking setting, in which the model-testing time is eliminated by reading the corresponding benchmark model records directly, we compare the refinement efficiency by evaluating the average number of model-testings required for a method to achieve a target performance level (see Evaluation Metrics section). The MB-centric model selection methods are excluded because they have no model refinement phase. As shown in Tab. V, more than half of the trials fail to identify a comparable model within 100 model-testings. Compared with ML-based meth-

TABLE V: Comparison of the average number of iterations required to reach the performance of M-DESIGN after 50 iterations. Trials failing to reach the targets within 100 iterations are counted as 100 in the calculation. Lower is better. If a baseline fails on all 10 repeated trials, we mark it as  $\infty$ .

	Act.	Com.	Pho.	Cit.	CS	Cora	Corn.	DBLP	Pub.	Tex.	Wis.
Ra.	86.5	71.9	$\infty$	$\infty$	85.2	$\infty$	$\infty$	$\infty$	$\infty$	74.0	79.0
RL	98.2	80.7	92.4	$\infty$	67.8	94.2	92.7	$\infty$	$\infty$	61.6	91.2
EA	91.4	61.7	96.4	$\infty$	83.8	$\infty$	$\infty$	89.1	$\infty$	53.1	96.9
Gr.	95.3	92.3	87.9	82.2	89.7	97.5	$\infty$	$\infty$	$\infty$	96.2	<b>41.2</b>
AG.	$\infty$	$\infty$	$\infty$	$\infty$	52.8	$\infty$	$\infty$	$\infty$	$\infty$	52.0	89.7
AT.	$\infty$	$\infty$	65.3	$\infty$	54.6	<b>32.8</b>	$\infty$	$\infty$	$\infty$	79.8	$\infty$
De.	74.0	79.4	<b>49.2</b>	<b>15.4</b>	96.8	$\infty$	$\infty$	<b>3.0</b>	<b>3.0</b>	<b>40.6</b>	62.6

ods (upper 5 rows), MB-centric model refinement methods (lower 2 rows) exhibit better refinement efficiency by requiring substantially fewer model-testings. However, as revealed in Tab. III, they cannot handle OOD and are actually converging prematurely to local optima, unable to further improve their selection with the rest of the budgets. This limitation arises because these methods are primarily optimized for static model queries and rely on static task-similarity views. In contrast, M-DESIGN closely navigates the unseen model-performance landscape by adaptively weaving fine-grained modification knowledge and iteratively refining models, cheaply delivering near-optimal performance with the least model-testings.

We present the comparison of long-run model refinement trajectories in Fig. 6 and Fig. 10. First, the results show that M-DESIGN consistently outperforms all baselines in terms of final performance, demonstrating the overall effectiveness of our method. Besides, it achieves comparable early-stage refinement efficiency to the MB-centric baselines, which are tailored for efficient model selection, demonstrating that our method is also a solid choice under limited resources.

### C. Analysis of Knowledge Efficacy

The *knowledge efficacy* improvements of M-DESIGN in Sec. III, i.e., architecture knowledge weaving engine and adaptive task-similarity views, rely on (1) the *linearity assumption* of modification gains between similar tasks, (2) the *Gaussian assumption* used in the Bayesian update, and (3) the *local consistency* in modification behavior. In this section, we empirically validate these assumptions respectively.

TABLE VI: Ablation study of M-DESIGN variants with average Kendall rank correlation.

Method	Actor	Computers	Photo	CiteSeer	CS	Cora	Cornell	DBLP	PubMed	Texas	Wisconsin	Avg Kendall Corr.
M-DESIGN	<b>34.89</b>	<b>89.22</b>	94.62	<b>74.59</b>	95.16	<b>88.50</b>	<b>77.48</b>	<b>84.29</b>	<b>89.08</b>	<b>83.79</b>	<b>91.33</b>	<b>0.34</b>
w/o windows	<b>34.89</b>	<b>89.22</b>	94.60	<b>74.59</b>	95.06	<b>88.50</b>	75.68	<b>84.29</b>	88.66	81.98	<b>91.33</b>	0.27
w/o dynamic	33.71	88.42	94.49	73.99	95.06	88.13	75.68	83.68	88.44	81.98	90.67	0.08
w/o OOD	<b>34.89</b>	88.42	<b>94.75</b>	<b>74.59</b>	<b>95.33</b>	<b>88.50</b>	75.68	<b>84.29</b>	<b>89.08</b>	81.98	90.67	0.31

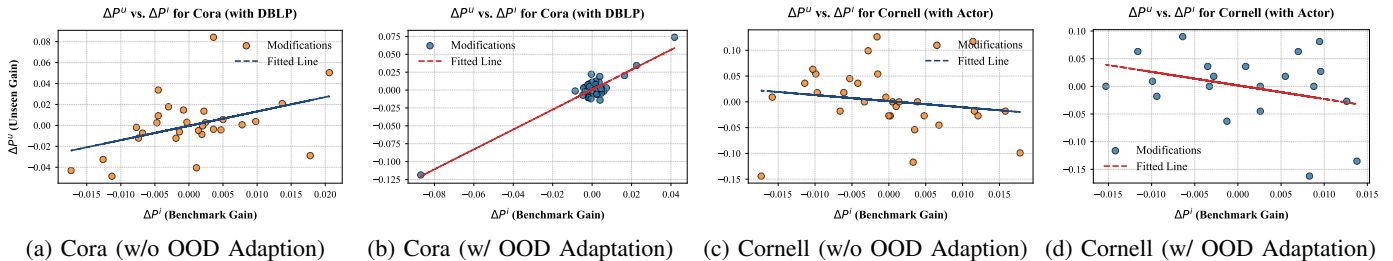


Fig. 7: Scatter plots showing benchmark modification gains (most similar benchmark dataset) vs. unseen modification gains for In-Dist. Cora (left) and Out-of-Dist. Cornell (right). Each dataset has results for two methods: w/ and w/o OOD adaptation.

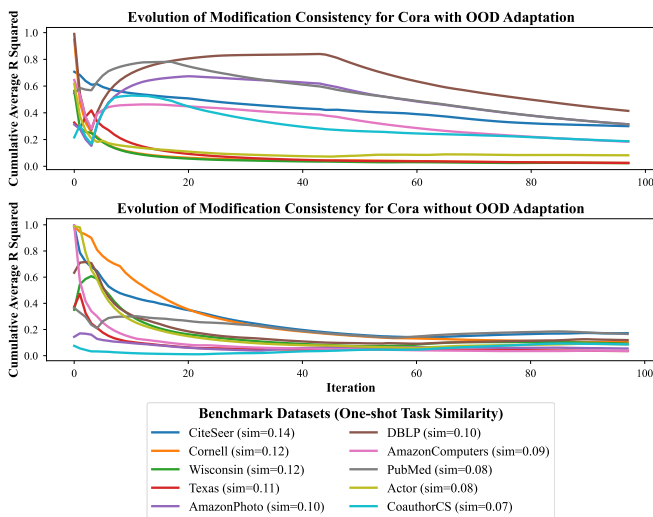


Fig. 8: Accumulated modification consistency on Cora dataset with (top) and without OOD adaptation (bottom).

1) *Validation of Assumptions:* Our theoretical formulation in Def. (2) and Eq. (15) relies on the *linearity assumption* and the *Gaussian assumption*. We present our assumption validations on Cora and Cornell for detailed illustration, which represent in-distribution and out-of-distribution, respectively.

As shown in Fig. 5, to quantify the linearity and normality, we report  $R^2$  and apply the Shapiro-Wilk test [63] by comparing the local modification gains of all benchmark datasets with the unseen datasets. First, the high-similarity benchmark datasets—DBLP for Cora and Actor for Cornell—exhibit obviously higher linearity. This validates our assumption that architecture modifications with similar gains on  $D^i$  remain informative for  $D^u$ , justifying our motivation for knowledge weaving. Besides, the p-values with high-similarity benchmark datasets are greater than 0.05, confirming that our local modification gains follow a Gaussian distribution, supporting the probabilistic update mechanism in Eq. (15).

As shown in Fig. 7, we measure the correlation between local modification gains on the unseen dataset and its most

similar benchmark dataset after task-similarity views have stabilized. The regression results in Fig. 7 show a strong linear relationship ( $R^2 = 0.87$ ) between the local modification gains when the unseen dataset Cora is highly similar to the benchmark dataset DBLP. In this in-distribution case, the local modification gains on DBLP are highly predictive of the gains on Cora, easily approaching the optimal model on Cora with knowledge weaving in Def. (3). For the OOD dataset Cornell, the linear relationship is less pronounced ( $R^2 = 0.03$ ) without any OOD adaptation, but it improves a lot ( $R^2 = 0.11$ ) after equipping the predictive query planners and still reaches optimum in Tab. III (we will discuss more in Sec. V-D).

2) *Analysis of Local Modification Consistency:* A key advantage of M-DESIGN is its ability to adapt task-similarity views dynamically based on the newly observed modification landscape. To demonstrate the necessity of this adaptability, we assess local consistency in modification behavior and reveal its varying nature. We track how the actual similarity between datasets evolves over iterations and compare it with the static similarity fixed after initialization. Fig. 8 presents the ground truth of accumulated local modification consistency for Cora across iterations, showing that static similarities listed in the legend often diverge a lot from true modification behavior. In contrast, M-DESIGN dynamically updates task-similarity views to reflect local patterns of architecture tweaks, ensuring a more reliable knowledge query. In Tab. VI, we further quantify the Kendall rank correlation between real local consistency and different task similarity views, showing that our dynamic one—with sliding windows to control the locality—achieved the best. We perform hyperparameter tuning to determine the generally good window sizes of  $\sim 30$  and  $\sim 40$ —w/o and w/ OOD adaptation, respectively—across diverse datasets.

#### D. Analysis of Knowledge Adaptation and Quality

Here, we validate our corresponding contributions in terms of knowledge adaptation and quality from three aspects:

**Impact of OOD adaptation:** We address the OOD issue by constructing predictive query planners on modification gain graphs in Sec. IV-C. We conduct an ablation study on its

TABLE VII: Comparison of ML-based and MB-centric model selection methods under a maximum search budget of 100 model-testings across 11 link prediction datasets. The best results are **bolded**. \* marks reaching global optimum.

Method	Actor	Computers	Photo	CiteSeer	CS	Cora	Cornell	DBLP	PubMed	Texas	Wisconsin
<b>Space Optimum</b>	<b>74.75</b>	<b>93.61</b>	<b>94.44</b>	<b>77.66</b>	<b>90.26</b>	<b>78.56</b>	<b>76.77</b>	<b>86.68</b>	<b>85.55</b>	<b>73.15</b>	<b>71.77</b>
Random	73.76	93.26	93.94	74.24	89.38	76.66	73.84	85.48	83.13	68.70	68.98
RL	73.92	93.19	94.06	74.24	89.26	76.40	73.38	85.37	83.60	69.07	68.30
EA	73.88	92.89	94.17	74.00	89.30	75.22	74.60	85.54	83.76	68.52	68.68
GraphNAS	73.97	93.04	93.99	74.18	89.48	76.30	74.40	85.75	83.87	69.95	68.47
Auto-GNN	74.58	93.34	94.08	74.68	89.46	74.09	75.36	85.10	82.86	70.18	69.93
GraphGym	72.35	86.70	93.00	71.91	87.63	70.88	69.19	85.00	74.88	66.67	66.33
NAS-Bench-Graph	70.33	92.94	93.00	71.91	87.63	70.88	64.14	84.46	82.54	66.67	66.67
AutoTransfer	74.65	<b>93.61*</b>	93.98	73.35	90.13	75.83	74.75	85.75	84.86	<b>73.15*</b>	70.07
DesiGNN	<b>74.75*</b>	<b>93.61*</b>	94.33	<b>75.11</b>	<b>90.26*</b>	75.67	<b>76.77*</b>	86.56	<b>85.55*</b>	71.29	<b>71.77*</b>
<b>M-DESIGN</b>	<b>74.75*</b>	<b>93.61*</b>	<b>94.44*</b>	74.98	<b>90.26*</b>	<b>78.56*</b>	<b>76.77*</b>	<b>86.68*</b>	<b>85.55*</b>	<b>73.15*</b>	<b>71.77*</b>

TABLE VIII: Comparison of ML-based and MB-centric model selection methods under a maximum search budget of 100 model-testings across 11 lgraph classification datasets. The best results are **bolded**. \* marks reaching global optimum.

Method	COX2	DD	IMDB-BINARY	IMDB-MULTI	NCII	NCII09	PROTEINS	PTC_FM	PTC_FR	PTC_MM	PTC_MR
<b>Space Optimum</b>	<b>86.74</b>	<b>80.43</b>	<b>81.00</b>	<b>48.56</b>	<b>80.82</b>	<b>78.83</b>	<b>79.73</b>	<b>70.53</b>	<b>68.57</b>	<b>73.63</b>	<b>66.67</b>
Random	85.24	79.86	79.98	47.33	78.82	77.47	78.53	69.04	66.71	69.90	62.11
RL	84.80	79.22	80.08	47.65	78.27	76.71	78.92	69.18	66.10	70.55	61.52
EA	84.77	79.16	79.28	47.29	78.33	77.49	78.67	68.75	65.76	69.06	61.13
GraphNAS	85.20	79.57	80.00	47.32	78.26	76.75	78.83	68.70	66.47	70.20	61.42
Auto-GNN	85.41	79.69	79.12	46.97	77.73	76.24	77.69	68.12	65.05	70.50	59.36
GraphGym	72.76	73.90	72.17	46.56	74.49	69.25	76.13	65.22	59.05	59.20	50.49
NAS-Bench-Graph	82.44	62.84	75.83	44.67	74.49	69.25	77.63	47.34	63.34	58.70	54.90
AutoTransfer	<b>86.74*</b>	78.44	80.17	47.22	79.00	77.74	78.38	67.15	<b>67.14</b>	70.15	61.76
DesiGNN	84.95	79.04	80.73	47.44	78.95	77.58	<b>79.73*</b>	69.09	<b>67.14</b>	70.55	62.25
<b>M-DESIGN</b>	<b>86.74*</b>	<b>80.14</b>	<b>81.00*</b>	<b>47.65</b>	<b>79.04</b>	<b>78.83*</b>	<b>79.73*</b>	<b>70.53*</b>	<b>67.14</b>	<b>73.63*</b>	<b>66.67*</b>

effectiveness across OOD datasets, including Computers, Cornell, and Texas. As shown in Tab. VI, removing OOD adaptation results in significant performance drops, particularly in Cornell. This validates that directly applying raw benchmark knowledge without adaptation can lead to negative transfer, reinforcing our contribution of predictive online adaptation.

**How OOD affects local modification consistency:** We evaluate such impact by studying the linearity in modification gains between known and unseen datasets. In Fig. 7, we observe that the linear correlation between modification gains is negligible (e.g., Cornell:  $R^2 = 0.03$ ) without OOD adaptation. However, our OOD adaptation successfully shifts the modification landscape, improving the correlation ( $R^2 = 0.11$ ). Furthermore, in Fig. 8, it is evident that after equipping the OOD adaptation, all the ground truth modification consistencies increase. This adaptation mechanism ensures that M-DESIGN remains effective and robust even under significant distribution shifts.

**Model space quality:** We show that our model space is better than NAS-Bench-Graph [35] in Tab. II.

In Tab. VI, we present the ablation study of removing OOD adaptation, dynamic task-similarity views, and sliding window.

### E. Parameter Sensitivity on Task Similarity Initialization

We conduct a parameter sensitivity study to investigate the impact of similarity threshold  $\delta_0$  and different task similarity initialization strategies based on the averaged performance of M-DESIGN across datasets. As discussed in Sec. IV-D, this includes 1) our average Kendall’s  $\tau$  rank correlation over

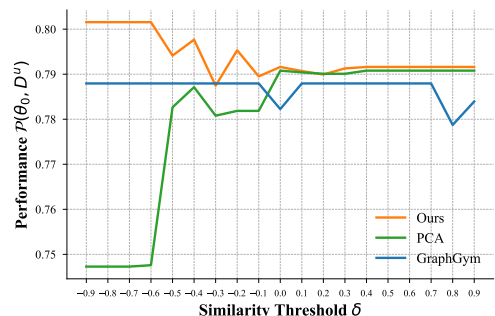


Fig. 9: Averaged performance of M-DESIGN under different task similarity initialization strategies and threshold  $\delta_0$ .

data statistic, 2) PCA initialization [56], and 3) GraphGym’s Kendall Tau initialization [26]. The results in Fig. 9 show that our ranking-based initialization consistently outperforms the other methods across all thresholds. Besides, we observe a highly favorable insensitive behavior in our method: its effectiveness increases with lower similarity thresholds  $\delta_0$ , indicating that M-DESIGN can adaptively utilize a broader set of benchmark datasets’ knowledge to select better models for new task datasets. Based on this observation, we safely remove the similarity threshold  $\delta_0$  in our final implementation to maximize the utilization of the model knowledge base.

### F. Generalizability of M-DESIGN Beyond the Graph Domain

To evaluate the generalizability of M-DESIGN and demonstrate the broader applicability, we conduct two additional instantiations in the tabular and image domains.

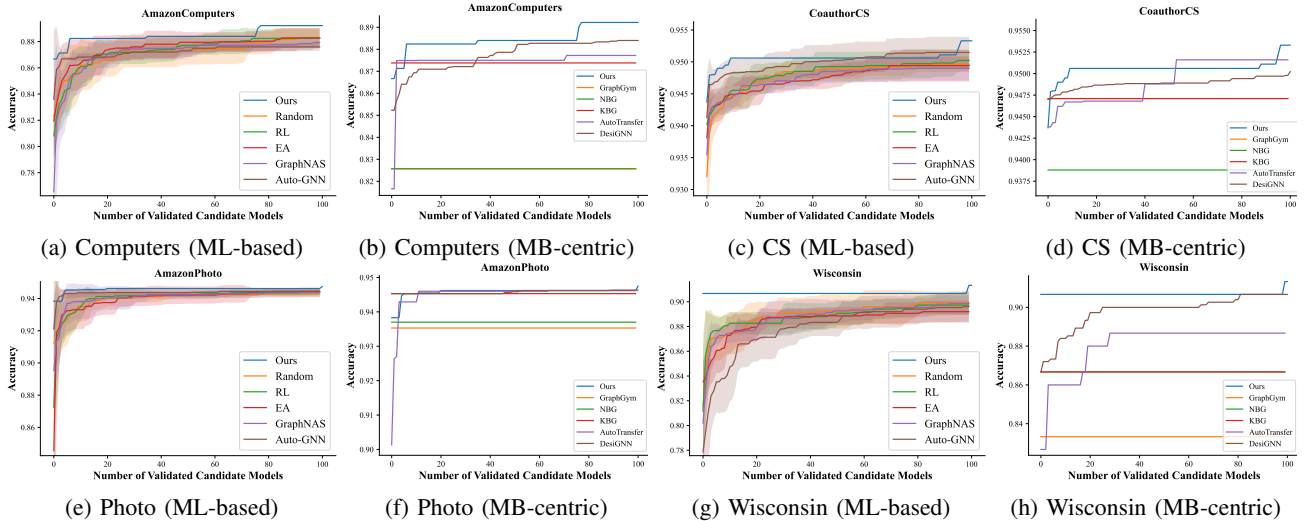


Fig. 10: Long-run model refinement trajectories of M-DESIGN compared to ML-based and MB-centric methods.

TABLE IX: Performance comparison of model refinement for data-sensitive tabular domain within 100 model-testings.

Method	Protein	Slice	Parkinson	Naval
<b>Optimal</b>	0.215368	0.000144	0.004239	0.000029
<b>Random</b>	0.260853	0.000448	0.015955	0.000453
<b>EA</b>	0.251967	0.000671	0.016186	0.000110
<b>MBMS</b>	0.319117	0.000799	0.018600	0.000317
Model Rank	(8768/62208)	(2150/62208)	(1021/62208)	(1554/62208)
<b>M-DESIGN-S</b>	<b>0.223902</b>	<b>0.000221</b>	<b>0.012643</b>	<b>0.000034</b>
Model Rank	<b>(29/62208)</b>	<b>(48/62208)</b>	<b>(294/62208)</b>	<b>(6/62208)</b>

TABLE X: M-DESIGN achieves outstanding results even without refinement in the data-insensitive image domain.

Method	Protein	Slice	Parkinson
<b>Optimal</b>	0.8916	0.6118	0.3827
<b>M-DESIGN-Init</b>	0.8896	0.6044	0.3827
Model Rank	<b>(6/15625)</b>	<b>(14/15625)</b>	<b>(1/15625)</b>

**Tabular Domain Instantiation.** Like graph data, M-DESIGN achieves outstanding results in the data-sensitive tabular domain. We instantiated M-DESIGN using HPOBench [64], a prominent hyperparameter optimization benchmark encompassing 4 tabular datasets with a total of 62,208 hyperparameter configurations. The performance metric is MSE. We implemented a classical MB-centric model selection (MBMS) that selects the best model from the dataset with the highest correlation in hyperparameter rank performance [26] (given in [64]). Our M-DESIGN-S implementation excludes task similarity initialization, window size control, and predictive query planners to quickly validate the generalizability of our knowledge weaving engine. We use  $(1st / \#total \text{ models})$  to denote model rank. As shown in Tab. IX, even this simplified version of M-DESIGN achieves highly competitive performance and ranking among the entire space of 62,208 configurations, significantly outperforming the baselines. These results affirm that M-DESIGN’s fundamental concept—leveraging dynamic

task-similarity views to weave modification knowledge from similar benchmark tasks for approximating the unseen landscape—can generalize effectively to other domains.

**Image Domain Instantiation.** For the image domain instantiation, we utilized the widely recognized NATS-Bench [65], encompassing 15,625 Convolutional Neural Networks (CNNs) evaluated across CIFAR-10, CIFAR-100, and ImageNet16-120 datasets. By using our Kendall’s  $\tau$  rank correlation over RGB statistics for task-similarity views and then transferring the best-performing model architecture, M-DESIGN directly delivers close-to-optimal architectures in one shot without additional model refinements in Tab. X, illustrating the ease of selecting models in uniform data modalities like images. These align perfectly with our selection of instantiation in the graph domain. i.e., the more heterogeneous nature of graph and tabular tasks imposes greater challenges and better demonstrates M-DESIGN’s strengths in effectively leveraging distinguishing task similarities and MKB-centric model refinement.

## VI. CONCLUSION

In this paper, we introduced M-DESIGN, a curated model knowledge base pipeline that elevates MB-centric methods from static model selection to fine-grained model refinement by adaptively weaving prior knowledge about model architecture modification. By addressing *knowledge efficacy* and *knowledge schema* issues, M-DESIGN effectively tackles the adaptive query problem behind complex model refinement, and adopts a graph-relational knowledge schema that enables fine-grained relational analytics over architecture tweaks, driving a predictive query planner to alleviate OOD issues. We release our structured model knowledge base—covering 3 graph tasks, 22 graph datasets, and 67,760 models in the graph learning domain—that explicitly models performance gains over architecture modifications across diverse tasks, further contributing to the database community. Overall, we hope that our work can pave the way for a refinement-oriented approach to MKB-centric model selection with high effectiveness.

## AI-GENERATED CONTENT ACKNOWLEDGEMENT

The authors confirm that the manuscript, including all text, figures, and experiments, was authored without the assistance of any AI tools. However, the accompanying code implementation includes an optional feature for initializing task similarity using a Large Language Model (LLM). This LLM-based initialization is provided as an implementation choice only and is not part of the main contributions of this work. All design, writing, and analysis were conducted by the authors.

## REFERENCES

- [1] F. Rosenblatt, "The perceptron: a probabilistic model for information storage and organization in the brain." *Psychological review*, vol. 65, no. 6, p. 386, 1958.
- [2] A. Vaswani, "Attention is all you need," *Advances in Neural Information Processing Systems*, 2017.
- [3] A. Krizhevsky, I. Sutskever, and G. E. Hinton, "Imagenet classification with deep convolutional neural networks," *Advances in neural information processing systems*, vol. 25, 2012.
- [4] K. He, X. Zhang, S. Ren, and J. Sun, "Deep residual learning for image recognition," in *Proceedings of the IEEE conference on computer vision and pattern recognition*, 2016, pp. 770–778.
- [5] T. N. Kipf and M. Welling, "Semi-supervised classification with graph convolutional networks," *arXiv preprint arXiv:1609.02907*, 2016.
- [6] J. Devlin, M.-W. Chang, K. Lee, and K. Toutanova, "Bert: Pre-training of deep bidirectional transformers for language understanding," *arXiv preprint arXiv:1810.04805*, 2018.
- [7] B. Zoph, V. Vasudevan, J. Shlens, and Q. V. Le, "Learning transferable architectures for scalable image recognition," in *Proceedings of the IEEE conference on computer vision and pattern recognition*, 2018, pp. 8697–8710.
- [8] H. Pham, M. Guan, B. Zoph, Q. Le, and J. Dean, "Efficient neural architecture search via parameters sharing," in *International conference on machine learning*. PMLR, 2018, pp. 4095–4104.
- [9] E. LeDell and S. Poirier, "H2o automl: Scalable automatic machine learning," in *Proceedings of the AutoML Workshop at ICML*, vol. 2020. ICML San Diego, CA, USA, 2020.
- [10] K. Zhou, X. Huang, Q. Song, R. Chen, and X. Hu, "Auto-gnn: Neural architecture search of graph neural networks," *Frontiers in big Data*, vol. 5, p. 1029307, 2022.
- [11] W. Wang, M. Zhang, G. Chen, H. Jagadish, B. C. Ooi, and K.-L. Tan, "Database meets deep learning: Challenges and opportunities," *ACM Sigmod Record*, vol. 45, no. 2, pp. 17–22, 2016.
- [12] M. Boehm, S. Tatikonda, B. Reinwald, P. Sen, Y. Tian, D. R. Burdick, and S. Vaithyanathan, "Hybrid parallelization strategies for large-scale machine learning in systemml," *Proceedings of the VLDB Endowment*, vol. 7, no. 7, pp. 553–564, 2014.
- [13] W. Wang, J. Gao, M. Zhang, S. Wang, G. Chen, T. K. Ng, B. C. Ooi, J. Shao, and M. Reyad, "Rafiki: machine learning as an analytics service system," *Proceedings of the VLDB Endowment*, vol. 12, no. 2, pp. 128–140, 2018.
- [14] C. Aberger, A. Lamb, K. Olukotun, and C. Ré, "Levelheaded: A unified engine for business intelligence and linear algebra querying," in *2018 IEEE 34th International Conference on Data Engineering (ICDE)*. IEEE, 2018, pp. 449–460.
- [15] J. V. D'silva, F. De Moor, and B. Kemme, "Aida: Abstraction for advanced in-database analytics," *Proceedings of the VLDB Endowment*, vol. 11, no. 11, pp. 1400–1413, 2018.
- [16] M. Stonebraker, P. Brown, D. Zhang, and J. Becla, "Scidb: A database management system for applications with complex analytics," *Computing in Science & Engineering*, vol. 15, no. 3, pp. 54–62, 2013.
- [17] Z. Luo, S. Cai, J. Gao, M. Zhang, K. Y. Ngiam, G. Chen, and W.-C. Lee, "Adaptive lightweight regularization tool for complex analytics," in *2018 IEEE 34th International Conference on Data Engineering (ICDE)*. IEEE, 2018, pp. 485–496.
- [18] S. S. Sandha, W. Cabrera, M. Al-Kateb, S. Nair, and M. Srivastava, "In-database distributed machine learning: demonstration using teradata sql engine," *Proceedings of the VLDB Endowment*, vol. 12, no. 12, 2019.
- [19] X. Li, B. Cui, Y. Chen, W. Wu, and C. Zhang, "Mlog: Towards declarative in-database machine learning," *Proceedings of the VLDB Endowment*, vol. 10, no. 12, pp. 1933–1936, 2017.
- [20] K. Kara, K. Eguro, C. Zhang, and G. Alonso, "Columnml: Column-store machine learning with on-the-fly data transformation," *Proceedings of the VLDB Endowment*, vol. 12, no. 4, pp. 348–361, 2018.
- [21] B. C. Ooi, S. Cai, G. Chen, Y. Shen, K.-L. Tan, Y. Wu, X. Xiao, N. Xing, C. Yue, L. Zeng *et al.*, "Neurdb: an ai-powered autonomous data system," *Science China Information Sciences*, vol. 67, no. 10, p. 200901, 2024.
- [22] X.-Z. Wu, W. Xu, S. Liu, and Z.-H. Zhou, "Model reuse with reduced kernel mean embedding specification," *IEEE Transactions on Knowledge and Data Engineering*, vol. 35, no. 1, pp. 699–710, 2023.
- [23] H. Miao, A. Li, L. S. Davis, and A. Deshpande, "Modelhub: Towards unified data and lifecycle management for deep learning," *arXiv preprint arXiv:1611.06224*, 2016.
- [24] M. Vartak, H. Subramanyam, W.-E. Lee, S. Viswanathan, S. Husnoo, S. Madden, and M. Zaharia, "Modeldb: a system for machine learning model management," in *Proceedings of the Workshop on Human-In-the-Loop Data Analytics*, 2016, pp. 1–3.
- [25] A. Kumar, R. McCann, J. Naughton, and J. M. Patel, "Model selection management systems: The next frontier of advanced analytics," *ACM SIGMOD Record*, vol. 44, no. 4, pp. 17–22, 2016.
- [26] J. You, Z. Ying, and J. Leskovec, "Design space for graph neural networks," *Advances in Neural Information Processing Systems*, vol. 33, pp. 17 009–17 021, 2020.
- [27] N. Xing, S. Cai, G. Chen, Z. Luo, B. C. Ooi, and J. Pei, "Database native model selection: Harnessing deep neural networks in database systems," *Proceedings of the VLDB Endowment*, vol. 17, no. 5, pp. 1020–1033, 2024.
- [28] L. Zeng, N. Xing, S. Cai, G. Chen, B. C. Ooi, J. Pei, and Y. Wu, "Powering in-database dynamic model slicing for structured data analytics," *arXiv preprint arXiv:2405.00568*, 2024.
- [29] Z. Li, H. Van Der Wilk, D. Zhan, M. Khosla, A. Bozzon, and R. Hai, "Model selection with model zoo via graph learning," in *2024 IEEE 40th International Conference on Data Engineering (ICDE)*. IEEE, 2024, pp. 1296–1309.
- [30] H. Liu, S. Di, J. Wang, Z. Wang, J. Wang, X. Zhou, and L. Chen, "Structuring benchmark into knowledge graphs to assist large language models in retrieving and designing models," in *The Thirteenth International Conference on Learning Representations*, 2025.
- [31] K. Cao, J. You, J. Liu, and J. Leskovec, "Autotransfer: Automl with knowledge transfer—an application to graph neural networks," *arXiv preprint arXiv:2303.07669*, 2023.
- [32] J. Wang, S. Di, H. Liu, Z. Wang, J. Wang, L. Chen, and X. Zhou, "Computation-friendly graph neural network design by accumulating knowledge on large language models," *arXiv preprint arXiv:2408.06717*, 2024.
- [33] Z. Wang, S. Di, and L. Chen, "A message passing neural network space for better capturing data-dependent receptive fields," in *Proceedings of the 29th ACM SIGKDD Conference on Knowledge Discovery and Data Mining*, 2023, pp. 2489–2501.
- [34] K. T. Chitty-Venkata, M. Emami, V. Vishwanath, and A. K. Somani, "Neural architecture search benchmarks: Insights and survey," *IEEE Access*, vol. 11, pp. 25 217–25 236, 2023.
- [35] Y. Qin, Z. Zhang, X. Wang, Z. Zhang, and W. Zhu, "Nas-bench-graph: Benchmarking graph neural architecture search," *Advances in neural information processing systems*, vol. 35, pp. 54–69, 2022.
- [36] X. He, K. Zhao, and X. Chu, "Automl: A survey of the state-of-the-art," *Knowledge-based systems*, vol. 212, p. 106622, 2021.
- [37] T. Li, J. Zhong, J. Liu, W. Wu, and C. Zhang, "Ease. ml: Towards multi-tenant resource sharing for machine learning workloads," *Proceedings of the VLDB Endowment*, vol. 11, no. 5, pp. 607–620, 2018.
- [38] S. Nakandala, Y. Zhang, and A. Kumar, "Cerebro: A data system for optimized deep learning model selection," *Proceedings of the VLDB Endowment*, vol. 13, no. 12, pp. 2159–2173, 2020.
- [39] Z.-H. Tan, J.-D. Liu, X.-D. Bi, P. Tan, Q.-C. Zheng, H.-T. Liu, Y. Xie, X.-C. Zou, Y. Yu, and Z.-H. Zhou, "Beimingwu: A learnware dock system," in *Proceedings of the 30th ACM SIGKDD Conference on Knowledge Discovery and Data Mining*, ser. KDD '24. New York, NY, USA: Association for Computing Machinery, 2024, p. 5773–5782. [Online]. Available: <https://doi.org/10.1145/3637528.3671617>
- [40] W. Jeong, H. Lee, G. Park, E. Hyung, J. Baek, and S. J. Hwang, "Task-adaptive neural network search with meta-contrastive learning," *Ad-*

- vances in *Neural Information Processing Systems*, vol. 34, pp. 21 310–21 324, 2021.
- [41] Y. Zhao, R. A. Rossi, and L. Akoglu, “Automatic unsupervised outlier model selection,” in *Proceedings of the 35th International Conference on Neural Information Processing Systems*, ser. NIPS ’21. Red Hook, NY, USA: Curran Associates Inc., 2021.
- [42] M. Zheng, X. Su, S. You, F. Wang, C. Qian, C. Xu, and S. Albanic, “Can gpt-4 perform neural architecture search?” *arXiv preprint arXiv:2304.10970*, 2023.
- [43] S. Zhang, C. Gong, L. Wu, X. Liu, and M. Zhou, “Automl-gpt: Automatic machine learning with gpt,” *arXiv preprint arXiv:2305.02499*, 2023.
- [44] T. Brown, B. Mann, N. Ryder, M. Subbiah, J. D. Kaplan, P. Dhariwal, A. Neelakantan, P. Shyam, G. Sastry, A. Askell *et al.*, “Language models are few-shot learners,” *Advances in neural information processing systems*, vol. 33, pp. 1877–1901, 2020.
- [45] H. Touvron, T. Lavril, G. Izacard, X. Martinet, M.-A. Lachaux, T. Lacroix, B. Rozière, N. Goyal, E. Hambro, F. Azhar *et al.*, “Llama: Open and efficient foundation language models,” *arXiv preprint arXiv:2302.13971*, 2023.
- [46] C. White, W. Neiswanger, and Y. Savani, “Bananas: Bayesian optimization with neural architectures for neural architecture search,” in *Proceedings of the AAAI conference on artificial intelligence*, vol. 35, no. 12, 2021, pp. 10 293–10 301.
- [47] B. Zoph, “Neural architecture search with reinforcement learning,” *arXiv preprint arXiv:1611.01578*, 2016.
- [48] M. Shi, Y. Tang, X. Zhu, Y. Huang, D. Wilson, Y. Zhuang, and J. Liu, “Genetic-gnn: Evolutionary architecture search for graph neural networks,” *Knowledge-based systems*, vol. 247, p. 108752, 2022.
- [49] H. Liu, K. Simonyan, and Y. Yang, “Darts: Differentiable architecture search,” 2019. [Online]. Available: <https://arxiv.org/abs/1806.09055>
- [50] T. Elsken, J. H. Metzen, and F. Hutter, “Neural architecture search: A survey,” *Journal of Machine Learning Research*, vol. 20, no. 55, pp. 1–21, 2019.
- [51] B. M. Oloulade, J. Gao, J. Chen, T. Lyu, and R. Al-Sabri, “Graph neural architecture search: A survey,” *Tsinghua Science and Technology*, vol. 27, no. 4, pp. 692–708, 2021.
- [52] C. Antonio, “Sequential model based optimization of partially defined functions under unknown constraints,” *Journal of Global Optimization*, vol. 79, no. 2, pp. 281–303, 2021.
- [53] P. I. Frazier, “Bayesian optimization,” in *Recent advances in optimization and modeling of contemporary problems*. Informs, 2018, pp. 255–278.
- [54] Y. Wang, Y. Sun, Z. Liu, S. E. Sarma, M. M. Bronstein, and J. M. Solomon, “Dynamic graph cnn for learning on point clouds,” *ACM Transactions on Graphics (tog)*, vol. 38, no. 5, pp. 1–12, 2019.
- [55] J. Shen, Y. Qu, W. Zhang, and Y. Yu, “Wasserstein distance guided representation learning for domain adaptation,” in *Proceedings of the AAAI conference on artificial intelligence*, vol. 32, no. 1, 2018.
- [56] K. Pearson, “Liii. on lines and planes of closest fit to systems of points in space,” *The London, Edinburgh, and Dublin philosophical magazine and journal of science*, vol. 2, no. 11, pp. 559–572, 1901.
- [57] L. Li and A. Talwalkar, “Random search and reproducibility for neural architecture search,” in *Uncertainty in artificial intelligence*. PMLR, 2020, pp. 367–377.
- [58] E. Real, A. Aggarwal, Y. Huang, and Q. V. Le, “Regularized evolution for image classifier architecture search,” in *Proceedings of the aaai conference on artificial intelligence*, vol. 33, no. 01, 2019, pp. 4780–4789.
- [59] Y. Gao, H. Yang, P. Zhang, C. Zhou, and Y. Hu, “Graph neural architecture search,” in *International joint conference on artificial intelligence*. International Joint Conference on Artificial Intelligence, 2021.
- [60] A. Paszke, S. Gross, F. Massa, A. Lerer, J. Bradbury, G. Chanan, T. Killeen, Z. Lin, N. Gimeshein, L. Antiga *et al.*, “Pytorch: An imperative style, high-performance deep learning library,” *Advances in neural information processing systems*, vol. 32, 2019.
- [61] H. Chase, “LangChain,” Oct. 2022. [Online]. Available: <https://github.com/langchain-ai/langchain>
- [62] M. Fey and J. E. Lenssen, “Fast graph representation learning with pytorch geometric,” *arXiv preprint arXiv:1903.02428*, 2019.
- [63] S. S. Shapiro and M. B. Wilk, “An analysis of variance test for normality (complete samples),” *Biometrika*, vol. 52, no. 3-4, pp. 591–611, 1965.
- [64] A. Klein and F. Hutter, “Tabular benchmarks for joint architecture and hyperparameter optimization,” *arXiv preprint arXiv:1905.04970*, 2019.
- [65] X. Dong, L. Liu, K. Musial, and B. Gabrys, “Nats-bench: Benchmarking nas algorithms for architecture topology and size,” *IEEE transactions on pattern analysis and machine intelligence*, vol. 44, no. 7, pp. 3634–3646, 2021.